

# Journal of Visualized Experiments

## LDL Cholesterol Uptake Assay Using Live Cell Imaging Analysis with Cell Health Monitoring

--Manuscript Draft--

<b>Article Type:</b>	Invited Methods Article - JoVE Produced Video
<b>Manuscript Number:</b>	JoVE58564R2
<b>Full Title:</b>	LDL Cholesterol Uptake Assay Using Live Cell Imaging Analysis with Cell Health Monitoring
<b>Keywords:</b>	Low Density Lipoprotein, LDLR, LDL Influx, LDL uptake, Dynasore, PCSK9, Simvastatin, Dynamin, Lipids, Cholesterol, Atherosclerosis.
<b>Corresponding Author:</b>	Lina Shehadeh University of Miami School of Medicine Miami, Florida UNITED STATES
<b>Corresponding Author's Institution:</b>	University of Miami School of Medicine
<b>Corresponding Author E-Mail:</b>	lshehadeh@med.miami.edu
<b>Order of Authors:</b>	Portia Ritter Keyvan Yousefi Juliana Ramirez Derek Dykxhoorn Armando Mendez Lina Shehadeh
<b>Additional Information:</b>	
<b>Question</b>	<b>Response</b>
Please indicate whether this article will be Standard Access or Open Access.	Open Access (US\$4,200)
Please indicate the <b>city, state/province, and country</b> where this article will be <b>filmed</b> . Please do not use abbreviations.	1501 NW 10TH AVE, Miami, Florida 33136

University of Miami  
1501 NW 10th Ave  
Miami, FL33136, USA  
305-243-0867  
lshehadeh@med.miami.edu

Dr. Indrani Mukherjee  
Science Editor  
*JoVE*

8/2/2018

Dear Dr. Mukherjee:

We are pleased to submit the revised version of an original methods article entitled “LDL Cholesterol Uptake Assay Using Live Cell Imaging Analysis with Cell Health Monitoring” for your consideration for publication in *JoVE*. Our improved LDL uptake assay using live cell imaging provides a sensitive platform to serially quantify LDL uptake at different time points in various human cell lines. Concurrently with LDL uptake measurements, this technique allows for monitoring of the cell health and growth in real time; therefore, it could be a useful tool for monitoring potential cytotoxicity in studies screening for compounds regulating cholesterol metabolism. We have validated our method in three relevant cell lines including human hepatic carcinoma (HepG2) cells, human renal epithelial (HK2) cells, and human coronary artery endothelial cells (HCAECs), suggesting the broad applicability of the technique. Moreover, our findings support the validity and sensitivity of the LDL uptake quantifications as confirmed by the use of well-known LDL uptake inhibitors, Dynasore and PCSK9, as well as the LDL uptake stimulator Simvastatin.

We believe this manuscript will be of useful impact to the field of cholesterol metabolism, and therefore is appropriate for publication in the *JoVE*. This manuscript has not been published and is not under consideration for publication elsewhere. We have no conflicts of interest to disclose.

Thank you for your consideration!

Sincerely,

**Lina Shehadeh, Ph.D., FAHA**

Assistant Professor of Medicine

Division of Cardiology

Interdisciplinary Stem Cell Institute

Director of the Cardiovascular Module for the MD and MD/MPH programs

University of Miami Leonard M. Miller School of Medicine

1501 NW 10th Ave, BRB 848 Suite FG (Lab), BRB 818 (Office)

Miami, FL 33136

Office Tel: 305-243-0867

**TITLE:****LDL Cholesterol Uptake Assay Using Live Cell Imaging Analysis with Cell Health Monitoring****AUTHORS & AFFILIATIONS:**

Portia Ritter<sup>1,2\*</sup>, Keyvan Yousefi<sup>1,3\*</sup>, Juliana Ramirez<sup>4</sup>, Derek M Dykxhoorn<sup>4,5</sup>, Armando J Mendez<sup>6</sup>, and Lina A Shehadeh<sup>\*1,2,7,8</sup>.

<sup>1</sup>Interdisciplinary Stem Cell Institute, University of Miami Leonard M. Miller School of Medicine, Miami, Florida, USA.

<sup>2</sup>Department of Medicine, Division of Cardiology, University of Miami Leonard M. Miller School of Medicine, Miami, Florida, USA.

<sup>3</sup>Department of Molecular and Cellular Pharmacology, University of Miami Leonard M. Miller School of Medicine, Miami, Florida, USA.

<sup>4</sup>Dr. John T. Macdonald Foundation Department of Human Genetics, University of Miami Leonard M. Miller School of Medicine, Miami, Florida, USA.

<sup>5</sup>John P. Hussman Institute for Human Genomics, University of Miami Leonard M. Miller School of Medicine, Miami, Florida, USA.

<sup>6</sup>Department of Medicine, Division of Endocrinology, Metabolism and Endocrinology and the Diabetes Research Institute, University of Miami Leonard M. Miller School of Medicine, Miami, Florida, USA.

<sup>7</sup>Vascular Biology Institute, University of Miami Leonard M. Miller School of Medicine, Miami, Florida, USA.

<sup>8</sup>Peggy and Harold Katz Family Drug Discovery Center, University of Miami Leonard M. Miller School of Medicine, Miami, Florida, USA.

\*These 2 authors contributed equally

**Corresponding Author:**

Lina A. Shehadeh (lshehadeh@med.miami.edu)  
Tel.: (305) 243-0867;

**Email Addresses of Co-authors:**

Portia Ritter (par125@med.miami.edu)  
Keyvan Yousefi (k1@miami.edu)  
Juliana Ramirez (DDykxhoorn@med.miami.edu)  
Derek M Dykxhoorn (DDykxhoorn@med.miami.edu)  
Armando J Mendez (amendez2@med.miami.edu)

**KEYWORDS:**

Low density lipoprotein, LDLR, LDL influx, LDL uptake, Dynasore, Simvastatin, recombinant PCSK9, dynamin, lipids, cholesterol, atherosclerosis.

**SUMMARY:**

This protocol provides an efficient approach to measuring LDL cholesterol uptake with real time influx rates using a live cell imaging system in various cell types. This technique provides a platform to screen the pharmacological activity of compounds affecting LDL influx while monitoring for cell morphology and hence potential cytotoxicity.

#### **ABSTRACT:**

The regulation of LDL cholesterol uptake through LDLR-mediated endocytosis is an important area of study in various major pathologies including metabolic disorder, cardiovascular disease, and kidney disease. Currently, there is no available method to assess LDL uptake while simultaneously monitoring for health of the cells. The current study presents a protocol, using a live cell imaging analysis system, to acquire serial measurements of LDL influx with concurrent monitoring for cell health. This novel technique is tested in three human cell lines (hepatic, renal tubular epithelial, and coronary artery endothelial cells) over a four-hour time course. Moreover, the sensitivity of this technique is validated with well-known LDL uptake inhibitors, Dynasore and recombinant PCSK9 protein, as well as by an LDL uptake promoter, Simvastatin. Taken together, this method provides a medium-to-high throughput platform for simultaneously screening pharmacological activity as well as monitoring of cell morphology, hence cytotoxicity of compounds regulating LDL influx. The analysis can be used with different imaging systems and analytical software.

#### **INTRODUCTION:**

The Low Density Lipoprotein Receptor (LDLR)-mediated LDL endocytosis is an important area of study since circulating LDL cholesterol levels are at the core of cardiovascular disease<sup>1</sup>, kidney disease<sup>2</sup> as well as a variety of inflammatory diseases<sup>3</sup> and genetic disorders with mutations in cholesterol transport genes<sup>4-7</sup>. Studies in LDLR-mediated cholesterol influx have led to identification of multiple research tools, such as Dynamin inhibitors including the chemical Dynasore<sup>8-10</sup>, as well as LDL-regulating proteins such as Proprotein Convertase Subtilisin/Kexin type 9 (PCSK9)<sup>11,12</sup>.

The LDL-LDLR endocytosis pathway begins with sequestering the LDL-LDLR complex on the cell surface into clathrin-coated pits<sup>13</sup>. Vesicles are then formed by invagination of the cell surface membrane internalizing the LDL-LDLR complex in vacuoles for transport inside the cell. As the formed vesicle matures into early and then late endosomes, the pH drops inside the late endosome, causing disassociation of the LDL from its receptor<sup>14</sup>. In the past, the methods of quantification of LDL influx depended on radio-labeled <sup>125</sup>I-LDL co-incubation with cells and subsequent extraction of the radio-labelled protein from cells for quantification<sup>15</sup>. This was then replaced by the use of fluorescently labelled LDL proteins such as Dil-LDL, and subsequent immunostaining or extraction of protein for fluorescent readings using a spectrophotometer or plate reader<sup>15,16</sup>. Fluorescently labelled LDL has also been used in Fluorescence-activated cell sorting (FACS) for analysis of internalization of LDL and cell surface LDL binding<sup>17</sup>. While these methods allow for collection of data after treatment, monitoring the viability of the cells during treatment is not possible.

The acidic pH in the late endosome allows the use of a pH-activated fluorescent LDL probe such



as pHrodo Red LDL that fluoresces after internalization<sup>18,19</sup>. This property allows for a continuous time course of LDL uptake assessment in live cells. Therefore, this protocol utilizes pHrodo Red-LDL fluorescence imaging in a live cell analysis to serially measure LDL uptake with concurrent monitoring for the cell health. The results indicate the reliability of this novel technique as tested over a four-hour time course in three different human cell lines, human hepatic carcinoma (HepG2) cells, human renal epithelial (HK2) cells and human coronary arterial endothelial cells (HCAEC). These cell lines are clinically significant to LDL clearance<sup>20-27</sup>, kidney disease<sup>28-31</sup>, and heart disease<sup>32,33</sup>, respectively. In addition to monitoring the LDL influx, this protocol incorporates treatment with two well-known LDL uptake inhibitors, Dynasore Hydrate and recombinant PCSK9 protein as well as a statin inducer of LDLR expression and LDL uptake, simvastatin. Dynasore and recombinant PCSK9 each work through different pathways to reduce LDL uptake.

Dynasore is a small molecule inhibitor of Dynamins<sup>10</sup> and reduces LDL uptake by blocking clathrin-dependent endocytosis of LDL-LDLR complex<sup>10,34</sup>. Recombinant PCSK9, on the other hand, is a member of peptidase S8 family that binds to LDLR and inhibits its recycling to the cell surface after releasing LDL from the internalized complex by blocking required conformational changes<sup>35,36</sup>. Decreased cell surface LDLR density eventually leads to reduced LDL uptake by the cell. Statins, while directly blocking the 3-hydroxy-3-methylglutaryl-coenzyme (HMG-CoA) reductase enzyme and thus cholesterol biosynthesis, are also known to upregulate the expression of LDLR<sup>25,38</sup> leading to increased LDL uptake. The sensitivity of this protocol is validated by detecting significant reductions in LDL influx in three clinically relevant human cell lines, HK2, HepG2 and HCAECs, by Dynasore and/or recombinant PCSK9, and a marked increase in LDL uptake in HepG2 cells by Simvastatin in a four-hour time course with monitoring for cell morphology/health. Taken together, this method provides a medium-to-high throughput platform for concurrently screening the pharmacological activity and cytotoxicity of compounds regulating LDL uptake in live cells.

## **PROTOCOL:**

### **1. Seeding Cells in a 24-well Plate**

1.1. Aspirate media off the cells, wash the cells with 5 mL of Dubelco's Phosphate Buffered Saline (dPBS), and aspirate the dPBS. For HepG2 cells in a 100 mm dish, use 1.5 mL of 0.25% Trypsin/EDTA, and for HK2 cells or HCAECs use 1.5 mL of 0.05% Trypsin/EDTA solution to detach the cells.

1.2. Incubate the plate in a 37 °C incubator for 4 minutes or until the cells are detached. Neutralize trypsin after a 4 minute incubation by adding 3 mL of complete media for HepG2 and HK2 or 3 mL of trypsin neutralizing solution, dPBS plus 5% fetal bovine serum (FBS), for HCAEC cells.

1.3. Transfer the cells into 15 mL conical tubes and centrifuge at 250 x g for 5 minutes, aspirate the media, and re-suspend the cell pellet in complete media.

1.4. Filter the cell suspension gently through a 40 µm mesh strainer to break up cell clumps. Do not wash the cells through the strainer.

1.5. Count the cells and plate them at an optimized density. For example, 5,000 cells per well of HepG2 cells or 10,000 cells per well of HK2 cells or HCAECs in a 24-well plate lead to optimal results.

1.6. Incubate the plate overnight at 37 °C to allow cells to attach.

1.7. The next day, change the cell media to base media for the cell line (without FBS) plus 5% Lipo-Protein Deficient Serum (LPDS) or low (2%) FBS media depending on the treatment (see 1.7). Then, continue incubation for 24 h to starve the cells. Use 500 µL of total media per well in a 24-well plate.

1.8. Treat the cells in one of three ways: Add 10 µg/mL of rPCSK9 (or vehicle) and return the cells to the 37 °C incubator for 1 hour, add 40 µM of Dynasore Hydrate (or vehicle, Dimethyl Sulfoxide) and return the cells to the 37 °C incubator for 10 minutes, or add 1 µM Simvastatin (or vehicle, Dimethyl Sulfoxide) and return the cells to the 37 °C incubator for 12, 18 or 24 hours. Use media with 5% LPDS for rPCSK9 or Dynasore treatments. Use low (2%) FBS media or media with 5% LPDS Simvastatin treatments.

Note: Treating the cells with desired compounds may be done at the time of media change for lipoprotein starvation (step 1.6) for long-term experiments, or prior to the analysis for short-term experiments. Alternatively, customized treatment times may be chosen based on the type and the purpose of the experiments.

1.9. Next, add 5 µL of pHrodo red-labelled LDL (1 mg/mL stock) to each well to obtain a final concentration of 10 µg/mL. Then, carefully remove any bubbles from the wells.

## 2. Live Cell Analysis

2.1. Immediately after adding the labelled LDL, place the plate in the live cell analysis system incubator (see **Table of Materials**) and allow the plate to equilibrate for 15 minutes to reduce condensation in the plate.

2.2. In the meantime, open the software and schedule the scan by adding the vessel holding the plate. Image 16 images per well at 1 hour intervals at 10X for 4 hours using the red and phase channels.

2.3. Create a Plate Map to use for data processing.

2.3.1. Click on the **Properties** tab. Choose the **Plate Map**. Input the cell type and treatments in **Compounds** tab.

2.3.2. Click on the **Regions** tab, select each set of replicates, and save as regions.

### 3. Set up Analysis Parameters

3.1. Once an experimental run is complete, create an Image Set in the software to train the computer to quantify each parameter included in the counting set.

3.1.1. In the software, open the plate view, then in the **Analysis Job Utilities** box choose **Create or Add to Image Collection**.

3.1.2. Select **New Image Collection**, type a name for the image collection, and choose the **Red** and **Phase** channels by checking the boxes next to the channels.

3.1.3. Select 5 more images and add to image collection by adding to the current image collection.

3.2. Create a Processing Definition for the cells. **Table 1** includes the parameters for the HepG2, HK2, and HCAE cell processing definitions for this LDL influx protocol.

3.2.1. In the **Analysis Job Utilities** box, choose **New Processing Definition**. Choose the Image Collection named in step 2.1.2 from the drop down menu. Input the parameters for the type of cells from **Table 1**.

3.2.2. In the **Preview** box, use the drop down menu to select **Preview All**.

3.2.3. In the **Analysis Mask** box, check the **Confluence Mask** and the **Red Object Mask** boxes to view the area included in the analysis for the processing definition. See **Figure 1**.

3.2.4. Scroll through the image collection to ensure the cells and LDL are included in the mask. Select **File** and **Save** the Processing Definition.

3.3. Analyze the set of images from the experimental run.

3.3.1. Open the experiment in plate view. In the **Analysis Job Utilities** box, choose **Launch New Analysis Job**. Select the saved Processing Definition.

3.3.2. Name the analysis job, choose the time range for analysis, and highlight the experimental wells to analyze. Click the **Launch** button.

### 4. Analysis and Data Processing

4.1. Once the Analysis Job is complete, export the data:

4.1.1. Select the completed analysis and press **View**. In the **Utilities** menu, choose **Metric/Graph Export**.

4.1.2. In the *Regions* menu, choose **All Wells**, and in the *Group* menu, to obtain the mean values for each set of wells as a group choose **Replicates** and for exporting the individual values for each well choose **None**.

4.1.3. In the **Red Object metric** menu, choose the **Total Red Object Integrated Intensity (RCU x  $\mu\text{m}^2/\text{image}$ )**. This parameter indicates the sum of the red signal intensity (in RCU) times the area of the red signal (in  $\mu\text{m}^2$ ) in all the images across each well, which corresponds to the total LDL uptake by the cells.

4.1.4. Click the **Data Export** button. Check **Break data down into individual images**. The data is automatically copied on a clipboard and can be pasted to a new spreadsheet file.

4.1.5. In the **Phase Object metric** menu, choose the **Confluence (Percent)**. Check **Break data down into individual images**. Click the **Data Export** button. The data is automatically copied on a clipboard and can be copied to the spreadsheet file containing Total Red Object Integrated Intensity data.

4.1.6. Apply the conversion of the percent confluence to total area with the following equation.

Total Phase Area ( $\mu\text{m}^2/\text{image}$ ) = Confluence (%)  $\times$  (Image Height (Pixels)  $\times$  Resolution)  $\times$  (Image Width (Pixels)  $\times$  Resolution)

**Note:** The confluence (%) parameter indicates the percent confluence of the phase area per image that corresponds to the area of the cells in each well. This metric should be converted into total phase area for each individual image once exported. The image specifications for phase channel (image height, width and resolution) to be used with the above formula for each experimental vessel can be found by referring to **Vessel Properties** under **Image Channels**.

4.1.7. Normalize Total Red Object Integrated Intensity to the Total Phase Area as calculated in 4.1.6 using the following formula for each individual image to eliminate the variability in the cell density across the wells.

4.1.7.1. Divide the **Total Red Object Integrated Intensity (RCU x  $\mu\text{m}^2/\text{image}$ )** values of each image by its corresponding **Total Phase Area ( $\mu\text{m}^2/\text{image}$ )** to obtain **LDL Uptake (RCU)** values per image.

4.1.7.2. Then, average the **LDL Uptake (RCU)** data of all images of each well to obtain the average LDL uptake in each well and then average the LDL uptake values of all the replicate wells to obtain group means. These data are the final LDL uptake values and may be used for illustration and statistical analysis using the software of choice.

## REPRESENTATIVE RESULTS:

### Live Cell Imaging Allows for Reliable Monitoring of Cell Health During Cholesterol Influx Studies in Three Human Cell Lines

We validated our assay in three human cell lines in which cholesterol homeostasis regulation plays a major pathophysiological role, including human hepatic carcinoma (HepG2) cells, human renal epithelial (HK2) cells, and human coronary artery endothelial cells (HCAECs). We used a live cell imaging system to perform the LDL uptake assay in a 4-hour time course with serial

measurements at 1-hour intervals. Our results indicate that all the cell types tested were compatible with this new technique and result in curves indicating continuous LDL uptake for the duration of the influx study with 4.33 hours as the final endpoint (**Figure 2**). The influx data shown in **Figure 2** were obtained by normalizing the total pHrodo Red-labeled LDL fluorescence (total red object integrated intensity per image in RCU x  $\mu\text{m}^2/\text{image}$ ) to the total cell area in each image of each well (phase object area per image in  $\mu\text{m}^2/\text{image}$ ) to eliminate the variability in the cell density across the wells. Furthermore, to validate the sensitivity of the LDL influx assay for the purpose of screening compounds affecting LDL cholesterol uptake, we used two positive controls known to inhibit LDL influx, Dynasore and rPCSK9, and one positive control known to induce LDL uptake, Simvastatin. As validated by our results, following treatment with Dynasore and rPCSK9, all three tested human cell lines (HepG2, HK2 and HCAEC) showed significant reductions in LDL influx over a 4-hour time course (**Figure 2A-C**). For example, **Figure 2A** shows that the LDL influx is reduced in HepG2 cells with treatment of Dynasore over the time course, compared to the cells treated with DMSO; while the DMSO as the vehicle control for Dynasore control had no significant effect on LDL influx compared to the untreated control group. Furthermore, our findings showed a marked increase in LDL uptake by HepG2 cells following treatment with Simvastatin (**Figure 3**), supporting the sensitivity of this method to detect significant alterations in the LDL influx. At about the 4.5 hour time point, which is a typical time point in LDL uptake studies, the LDL influx is significantly reduced with either Dynasore or rPCSK9 treatment, and increased by Simvastatin treatment (**Figure 4**).

A major advantage to using live cell imaging for LDL uptake studies is that this system provides real time images of the cells in each well that could be used to monitor potential cytotoxicity of the examined compounds. **Figures 5-7** illustrate representative images of the three cell lines investigated at the initial time point (0.33 h) and final endpoint (4.33 h) as a visual reference for the net LDL influx. The images confirm the normal morphology of the cells following Dynasore or rPCSK9 treatments, indicating both effectiveness and safety of these compounds.

### **Live Cell Analysis Gives Reliable Serial Quantitative Cholesterol Influx Measurements with Various Treatments**

A major advantage of using this protocol with a live cell imaging system is the ability to collect data throughout the time course and compare LDL influx at multiple time points rather than just one final time point as traditionally done. Using this protocol, we are able to calculate the percent reduction in LDL influx at the terminal time point as well as at 1 hour intervals throughout the time course. **Table 2** summarizes the reduction in LDL influx in three tested human cell lines following 10 min pre-treatment with 40  $\mu\text{M}$  Dynasore or 1 hour pre-treatment with 10  $\mu\text{g}/\text{mL}$  rPCSK9. At 4.33 hours as the final study end point, treatment with Dynasore at 40  $\mu\text{M}$  significantly reduced LDL influx in HepG2 cells, HK2 cells and HCAECs by 53%, 68% and 54%, respectively (**Table 2A-C**) and treatment with rPCSK9 at 10  $\mu\text{g}/\text{mL}$  resulted in 55% reduction in LDL influx in HK2 cells (**Table 2B**). In addition to quantifying the terminal time point as in traditional assays, we are able to perform a quantitative analysis in the reduction of LDL influx due to treatment at each time point of the experiment. For example, **Table 2B** shows that treatment with rPCSK9 in HK2 cells resulted in a reduction of LDL uptake by 79% at 1.33 hours, 67% at 2.33 hours, 59% at

3.33 hours post treatment compared to untreated cells. This protocol provides a reliable method for quantitative analysis of LDL influx after treatment.

#### FIGURE AND TABLE LEGENDS:

**Figure 1. Processing Definition Mask.** Representative images of HK2 cells are depicted following the application of the appropriate processing definition (detailed in **Table 1**). Shown are HK2 cells without masking (**A**), with Phase Mask applied (**B**), with Red Object Mask applied (**C**), or with both Phase and Red Object masks applied (**D**). Scale bar = 100  $\mu\text{m}$ .

**Figure 2. Reduction in LDL uptake using live cell imaging system over a 4.33 h time course.** Live cell analysis system is used to measure LDL influx in human hepatic carcinoma (HEPG2) cells (**A**), human renal tubular epithelial (HK2) cells (**B**), and human coronary artery endothelial (HCAE) cells (**C**). The cells were treated with Dynasore (10 minutes before the run) or rPCSK9 (one hour before the run) as positive controls. DMSO was used as a vehicle for Dynasore treatments. Positive controls significantly decreased the LDL influx in all 3 cell lines. LDL influx values were obtained by normalizing the total red object integrated intensity ( $\text{RCU} \times \mu\text{m}^2/\text{image}$ ) to the total phase object area ( $\mu\text{m}^2/\text{image}$ ). Data are mean  $\pm$  SEM. N = 6 wells/group. Data are representative of 2 or 3 independent experiments. \*\*\*\* $p < 0.0001$  vs blank, and ##### $p < 0.0001$  vs DMSO, using two-way ANOVA.

**Figure 3. Increase in LDL uptake using live cell imaging system over a 4.33h time course.** Live cell analysis system is used to measure LDL influx in human hepatic carcinoma (HEPG2) cells. LDL uptake is significantly increased following treatment with Simvastatin for 12 hours (**A**), 18 hours (**B**), or 24 hours (**C**) using media containing 2% FBS. The 24 hour time point was also performed with media containing 5% LPDS (without FBS). DMSO was used as negative control. LDL influx values were obtained by normalizing the total red object integrated intensity ( $\text{RCU} \times \mu\text{m}^2/\text{image}$ ) to the total phase object area ( $\mu\text{m}^2/\text{image}$ ). Data are mean  $\pm$  SEM. N = 6 wells/group. Data are representative of one independent experiment. \*\*\*\* $p < 0.0001$  vs DMSO, using Student's t-test.

**Figure 4. Significant LDL influx reduction by LDL uptake-lowering agents at 4.3 hour time point.** LDL influx is significantly reduced in human hepatic carcinoma (HepG2) cells (**A**), human renal tubular epithelial (HK2) cells (**B**), and human coronary artery endothelial (HCAE) cells (**C**) following treatment with LDL uptake inhibitors Dynasore for 10min or rPCSK9 for 1 hour. LDL influx is markedly increased by Simvastatin in HepG2 cells after 12, 18 or 24 hours treatments (**D**). Data are mean  $\pm$  SEM. N = 6 wells/group. Data are representative of 2 or 3 independent experiments. \*\*\*\* $p < 0.0001$  using two-way ANOVA.

**Figure 5. Reduced LDL influx in hepatocellular carcinoma (HepG2) cells by LDL uptake-lowering agent, Dynasore.** Representative images of the phase object and red object for HepG2 cells are depicted at 0.33 hour (left panels) and the 4.33 hour endpoint (right panels) show healthy status of cells. 40  $\mu\text{M}$  Dynasore, known to reduce LDL-cholesterol uptake, was used as positive control (**C**). Images were taken at 10X magnification. Scale bar = 100  $\mu\text{m}$ .

**Figure 6. Reduced LDL influx in human renal tubular epithelial (HK2) cells by LDL uptake-lowering agents, Dynasore and rPCSK9.**

Representative images of the phase object and red object for HK2 cells depicted at 0.33 hour (left panels) and the 4.33 hour endpoint (right panels) show healthy status of the cells. 40  $\mu$ M Dynasore (C), or 10  $\mu$ g/mL rPCSK9 (D), known to reduce LDL cholesterol uptake, were used as positive control. Images are taken at 10X magnification. Scale bar = 100  $\mu$ m.

**Figure 7. Reduced LDL influx in human coronary artery endothelial cells (HCAECs) by LDL uptake-lowering agent, Dynasore.**

Representative images of the phase object and red object for HCAECs depicted at 0.33 hour (left panels) and the 4.33 hour endpoint (right panels) show healthy status of the cells. 40  $\mu$ M Dynasore, known to reduce LDL-cholesterol uptake, was used as positive control (C). Images were taken at 10X magnification. Scale bar = 100  $\mu$ m. Data are mean $\pm$ SEM. N = 6 wells/group. Data are representative of 2 or 3 independent experiments.

**Table 1. Processing Definition Parameters.** These parameters are specific for the analysis system used in this protocol. Parameters should be set up to analyze red area in the red channel and the area of the cell in the phase channel. Parameter settings for HepG2, HK2, HCAE cell lines are presented.

**Table 2: Percent Change in LDL influx in HepG2, HK2 and HCAE cells treated with Dynasore, rPCSK9, or Simvastatin at 4.3 hours. A. HepG2 cells B. HK2 cells C. HCAE cells D. HepG2 cells.**

**DISCUSSION.**

In the current protocol, we demonstrate the utilization of live cell imaging as a new and more effective method for measuring real time LDL uptake over a time course in various human cell lines. Human hepatic carcinoma (HepG2) cells are commonly used in studies screening for cholesterol-lowering therapeutics<sup>21-26,39,40</sup>. Therefore, we chose this cell type for testing the capability of a live cell imaging system for LDL influx studies. Our results indicate that HepG2 cells are compatible with this new technique and result in a sigmoid-like curve indicating continuous LDL uptake for the duration of the influx assay until 4.33 hours as the final endpoint (**Figures 2A and 3**).

Cholesterol homeostasis plays a major role in the pathophysiology of various nephropathies. Indeed, cholesterol accumulation in renal tissue is a major contributor to renal fibrosis leading to chronic kidney disease and is a major pathology in various nephropathies<sup>28-31</sup>. Hence, we examined our method in human renal epithelial (HK2) cells as a popular and reliable cell line utilized in the field of nephrology. Our data also supported the feasibility of the live cell imaging system to measure LDL influx in HK2 cells. As shown in **Figure 2B**, HK2 cells took up LDL cholesterol linearly throughout the duration of the influx study (4 hours).

Due to the importance of the cholesterol metabolism in the development and progression of atherosclerosis<sup>32,33,41</sup>, the leading cause of cardiovascular disease, which in turn is the number-

one killer worldwide<sup>42</sup>, we aimed to validate our method in an atherosclerosis-relevant cell type. We used Human Coronary Arterial Endothelial Cells (HCAECs), as these are one of the first cell types to be exposed to a cholesterol insult in the coronary artery lumen of an atherosclerosis patient. Our data shown in **Figure 2C** indicates that this LDL influx method also works effectively with HCAECs. The resultant graph is a sigmoid-like curve similar to that of HepG2 cells.

To test the validity and sensitivity of this improved LDL influx assay for screening compounds affecting LDL-cholesterol uptake, we used three controls, LDL uptake-lowering agents Dynasore and rPCSK9, and LDL influx activator Simvastatin. Here, we treated the above mentioned cell lines (HepG2, HK2 and HCAECs) with optimized concentrations of Dynasore or rPCSK9 prior to the influx assay. Our results showed that all three tested cell lines responded to the treatments with significant reductions in LDL influx over a 4-hour time course (**Figure 2**). For instance, at 4.33 hours as the final time point, treatment with Dynasore at 40  $\mu$ M significantly reduced LDL influx in HepG2 cells, HK2 cells and HCAECs by 53%, 68% and 54%, respectively ( $p < 0.0001$ ; **Figure 2A-C** and **Table 2A-C**). In addition, rPCSK9 at 10  $\mu$ g/mL caused a marked 55% reduction in LDL influx in HK2 cells ( $p < 0.0001$ ; **Figure 2B** and **Table 2B**). Moreover, our findings showed that treating HepG2 cells with Simvastatin resulted in a marked increase in LDL uptake (**Figure 3**), supporting the sensitivity of this method to detect significant alterations in the LDL influx. Studies of treatment with rPCSK9 in HepG2 and HCAEC cells are not included in this protocol as rPCSK9 is used as an additional control treatment with well-documented results, but is costly to buy in small quantities. Therefore rPCSK9 was only used to validate this protocol in HK2 cells.

Live cell imaging analysis, along with the functional and timely measurement of LDL influx, allowed for continuous monitoring of the health and morphology of the cells. This advantage can efficiently detect potential cytotoxicity of the applied compounds, making this method an ideal technique for simultaneously monitoring pharmacological activity and cytotoxicity. **Figures 5-7** illustrate representative images of the three tested cell lines at the final endpoint (4.33 h) as a visual reference for the effect of the treatments on net LDL influx and also shows the healthy morphology of the cells following the tested treatments. We recommend visual inspection of all the images from each well to assure the healthy morphology of the cells for the duration of the study. For example, in data not shown, when images of HepG2 cells treated with 80  $\mu$ M Dynasore were inspected, we observed indications of cell detachment as the edges of the cells appeared to be lifting off the plate, suggesting cell detachment at higher concentrations of Dynasore. Furthermore, high concentrations of simvastatin (3-10  $\mu$ M) also led to altered morphology indicating induced apoptosis as reported for high dosages of statins<sup>45</sup>. This protocol was used to perform a titration of the Dynasore treatment at 20-80  $\mu$ M, and Simvastatin at 0.5-10  $\mu$ M concentration, following which the cell images were used to analyze the health of the cells and determine potential cytotoxicity of the treatments at various concentrations. Results suggested the use of 40  $\mu$ M for Dynasore and 1  $\mu$ M for simvastatin as optimal concentrations.

Lastly, we suggest performing a cell density titration study if another cell line is to be tested with this method in order to identify the optimal cell number per well to obtain consistent results. Our cell density optimization study showed that 10,000 cells/well in a 24-well plate lead to consistent LDL influx outcomes for HK2 and HCAEC cells. It is important to note that for this LDL influx assay



using live cell imaging system, a monolayer of non-confluent cells distributed evenly on the wells is desirable as clumps of cells may give rise to errors in the final normalized LDL influx values. The reason for this is that for the normalization of the influx data, the phase object area is used as a measure of cell density and this parameter can be adversely affected when cell clumps are formed. We observed that HepG2 cells have a tendency to form clumps when seeded at densities higher than 5,000 cells/well causing inconsistent influx results; therefore, we used 5,000 cells per well in a 24-well plate as optimal density for HepG2 cells.

Collectively, our method provides a medium-to-high throughput platform for screening the pharmacological activity and cytotoxicity of compounds regulating LDL influx concurrently. This method can be readily adapted for use with other fluorescently-labeled ligands that enter the lysosomal compartment to evaluate ligand uptake in real time. While this protocol offers specifications for Incucyte live imaging and analysis system, the protocol can be adapted for alternative imaging systems such as Cellomics.

#### ACKNOWLEDGMENTS:

This work was supported by the following grants to LAS: National Institute of Health (R56HL132209 and 1R01HL140468) and the Miami Heart Research Institute. KY is a recipient of American Heart Association Predoctoral Fellowship (18PRE33960070). HepG2 cells were kindly provided by Dr. Emmanuel Thomas, university of Miami-Miller School of Medicine<sup>46-48</sup>.

#### DISCLOSURES:

The authors declare that they have no competing financial interests.

#### REFERENCES:

- 1 Baigent, C. *et al.* Efficacy and safety of cholesterol-lowering treatment: prospective meta-analysis of data from 90,056 participants in 14 randomised trials of statins. *Lancet*. **366** (9493), 1267-1278, (2005).
- 2 Trevisan, R., Dodesini, A. R. & Lepore, G. Lipids and renal disease. *Journal of the American Society of Nephrology*. **17** (4 suppl 2), S145-S147, (2006).
- 3 Tall, A. R. & Yvan-Charvet, L. Cholesterol, inflammation and innate immunity. *Nature Reviews Immunology*. **15** (2), 104, (2015).
- 4 Dedoussis, G. V., Schmidt, H. & Genschel, J. LDL - receptor mutations in Europe. *Human Mutation*. **24** (6), 443-459, (2004).
- 5 Sasaki, K. *et al.* ATP-binding cassette transporter A subfamily 8 is a sinusoidal efflux transporter for cholesterol and taurocholate in mouse and human liver. *Molecular Pharmaceutics*. (2018).
- 6 Storch, J. & Xu, Z. Niemann–Pick C2 (NPC2) and intracellular cholesterol trafficking. *Biochimica et Biophysica Acta (BBA)-Molecular and Cell Biology of Lipids*. **1791** (7), 671-678, (2009).
- 7 Jansen, P. J. *et al.* Absence of ApoE upregulates murine brain ApoD and ABCA1 levels, but does not affect brain sterol levels, while human ApoE3 and human ApoE4 upregulate brain cholesterol precursor levels. *Journal of Alzheimer's Disease*. **18** (2), 319-329, (2009).

449 8 Girard, E. *et al.* The dynamin chemical inhibitor dynasore impairs cholesterol trafficking  
450 and sterol-sensitive genes transcription in human HeLa cells and macrophages. *PLoS One*.  
451 **6** (12), e29042, (2011).

452 9 Robinet, P. *et al.* Dynamin is involved in endolysosomal cholesterol delivery to the  
453 endoplasmic reticulum: role in cholesterol homeostasis. *Traffic*. **7** (7), 811-823, (2006).

454 10 Macia, E. *et al.* Dynasore, a cell-permeable inhibitor of dynamin. *Developmental Cell*. **10**  
455 (6), 839-850, (2006).

456 11 Benjannet, S. *et al.* NARC-1/PCSK9 and its natural mutants: zymogen cleavage and effects  
457 on the LDLR and LDL-cholesterol. *Journal of Biological Chemistry*. (2004).

458 12 Qian, Y.-W. *et al.* Secreted PCSK9 downregulates low density lipoprotein receptor through  
459 receptor-mediated endocytosis. *Journal of Lipid Research*. **48** (7), 1488-1498, (2007).

460 13 Brown, M. S. & Goldstein, J. L. A receptor-mediated pathway for cholesterol homeostasis.  
461 *Science*. **232** (4746), 34-47, (1986).

462 14 Goldstein, J. L. & Brown, M. S. History of discovery: the LDL receptor. *Arteriosclerosis,*  
463 *Thrombosis, and Vascular Biology*. **29** (4), 431, (2009).

464 15 Stephan, Z. F. & Yurachek, E. C. Rapid fluorometric assay of LDL receptor activity by Dil-  
465 labeled LDL. *Journal of Lipid Research*. **34** (2), 325-330, (1993).

466 16 Fisher, T. S. *et al.* Effects of pH and low density lipoprotein (LDL) on PCSK9-dependent LDL  
467 receptor regulation. *Journal of Biological Chemistry*. **282** (28), 20502-20512, (2007).

468 17 Atrahimovich, D., Khatib, S., Sela, S., Vaya, J. & Samson, A. O. Punicalagin induces serum  
469 low-density lipoprotein influx to macrophages. *Oxidative Medicine and Cellular Longevity*.  
470 **2016**, (2016).

471 18 Xu, M. *et al.*  $\delta$ -Tocopherol reduces lipid accumulation in Niemann-Pick type C1 and  
472 Wolman cholesterol storage disorders. *Journal of Biological Chemistry*. jbc. M112.  
473 357707, (2012).

474 19 Bonilla, D. L. *et al.* Autophagy regulates phagocytosis by modulating the expression of  
475 scavenger receptors. *Immunity*. **39** (3), 537-547, (2013).

476 20 Guo, M. *et al.* Apelin-13 Decreases Lipid Storage in Hypertrophic Adipocytes *In vitro*  
477 Through the Upregulation of AQP7 Expression by the PI3K Signaling Pathway. *Medical*  
478 *Science Monitor : International Medical Journal of Experimental and Clinical Research*. **20**  
479 1345-1352, (2014).

480 21 Guillemot, J., Asselin, M. C., Susan - Resiga, D., Essalmani, R. & Seidah, N. G.  
481 Deferoxamine stimulates LDLR expression and LDL uptake in HepG2 cells. *Molecular*  
482 *Nutrition & Food Research*. **60** (3), 600-608, (2016).

483 22 Javitt, N. B. Hep G2 cells as a resource for metabolic studies: lipoprotein, cholesterol, and  
484 bile acids. *The FASEB Journal*. **4** (2), 161-168, (1990).

485 23 Mullen, P. J., Lüscher, B., Scharnagl, H., Krähenbühl, S. & Brecht, K. Effect of simvastatin  
486 on cholesterol metabolism in C2C12 myotubes and HepG2 cells, and consequences for  
487 statin-induced myopathy. *Biochemical Pharmacology*. **79** (8), 1200-1209, (2010).

488 24 McNutt, M. C. *et al.* Antagonism of secreted PCSK9 increases low density lipoprotein  
489 receptor expression in HepG2 cells. *Journal of Biological Chemistry*. **284** (16), 10561-  
490 10570, (2009).

491 25 Scharnagl, H. *et al.* Effect of atorvastatin, simvastatin, and lovastatin on the metabolism  
492 of cholesterol and triacylglycerides in HepG2 cells. *Biochemical Pharmacology*. **62** (11),

1545-1555, (2001).

26 Scharnagl, H. *et al.* The effects of lificrol (K12. 148) on the cholesterol metabolism of cultured cells: evidence for sterol independent stimulation of the LDL receptor pathway. *Atherosclerosis*. **153** (1), 69-80, (2000).

27 Chan, J. C. *et al.* A proprotein convertase subtilisin/kexin type 9 neutralizing antibody reduces serum cholesterol in mice and nonhuman primates. *Proceedings of the National Academy of Sciences*. **106** (24), 9820-9825, (2009).

28 Ding, W. *et al.* Osteopontin deficiency ameliorates Alport pathology by preventing tubular metabolic deficits. *JCI Insight*. **3** (6), (2018).

29 Herman-Edelstein, M., Scherzer, P., Tobar, A., Levi, M. & Gafter, U. Altered renal lipid metabolism and renal lipid accumulation in human diabetic nephropathy. *Journal of Lipid Research*. **55** (3), 561-572, (2014).

30 Su, H. *et al.* Lipid Deposition in Kidney Diseases: Interplay Among Redox, Lipid Mediators, and Renal Impairment. *Antioxidants & Redox Signaling*. **28** (10), 1027-1043, (2018).

31 Agrawal, S., Zaritsky, J. J., Fornoni, A. & Smoyer, W. E. Dyslipidaemia in nephrotic syndrome: mechanisms and treatment. *Nature Reviews Nephrology*. **14** (1), 57, (2018).

32 Babiak, J. & Rudel, L. L. Lipoproteins and atherosclerosis. *Baillieres Clinical Endocrinology and Metabolism*. **1** (3), 515-550, (1987).

33 Wang, H. H., Garruti, G., Liu, M., Portincasa, P. & Wang, D. Cholesterol and Lipoprotein Metabolism and Atherosclerosis: Recent Advances in Reverse Cholesterol Transport. *Annals of Hepatology*. **16** (S1), 28-42, (2018).

34 Preta, G., Cronin, J. G. & Sheldon, I. M. Dynasore-not just a dynamin inhibitor. *Cell Communication and Signaling*. **13** (1), 24, (2015).

35 Horton, J. D., Cohen, J. C. & Hobbs, H. H. Molecular biology of PCSK9: its role in LDL metabolism. *Trends in Biochemical Sciences*. **32** (2), 71-77, (2007).

36 Abifadel, M. *et al.* Mutations in PCSK9 cause autosomal dominant hypercholesterolemia. *Nature Genetics*. **34** (2), 154, (2003).

37 Goldstein, J. L. & Brown, M. S. Regulation of the mevalonate pathway. *Nature*. **343** (6257), 425, (1990).

38 Dong, B., Wu, M., Cao, A., Li, H. & Liu, J. Suppression of Idol expression is an additional mechanism underlying statin-induced up-regulation of hepatic LDL receptor expression. *International Journal of Molecular Medicine*. **27** (1), 103-110, (2011).

39 Song, K. H., Kim, Y. H., Im, A.-R. & Kim, Y. H. Black Raspberry Extract Enhances LDL Uptake in HepG2 Cells by Suppressing PCSK9 Expression to Upregulate LDLR Expression. *Journal of Medicinal Food*. (2018).

40 Chan, J. C. *et al.* A proprotein convertase subtilisin/kexin type 9 neutralizing antibody reduces serum cholesterol in mice and nonhuman primates. *Proceedings of the National Academy of Sciences of the United States of America*. **106** (24), 9820-9825, (2009).

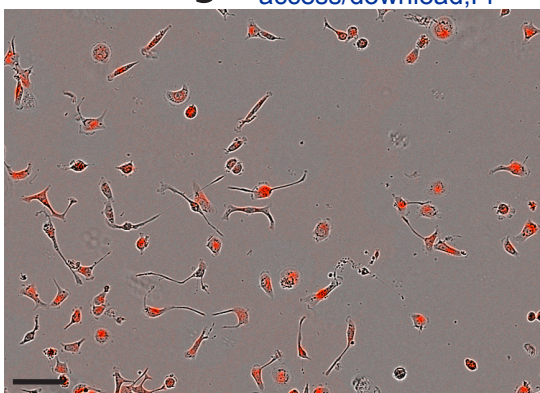
41 Tabas, I., Williams, K. J. & Borén, J. Subendothelial lipoprotein retention as the initiating process in atherosclerosis: update and therapeutic implications. *Circulation*. **116** (16), 1832-1844, (2007).

42 Benjamin, E. J. *et al.* Heart disease and stroke statistics-2017 update: a report from the American Heart Association. *Circulation*. **135** (10), e146-e603, (2017).

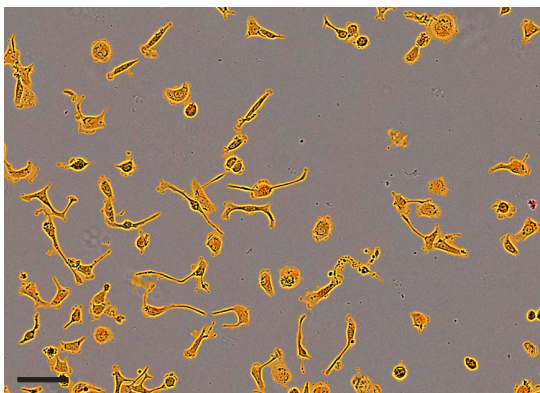
43 Brown, M. S. & Goldstein, J. L. The SREBP pathway: regulation of cholesterol metabolism

537 by proteolysis of a membrane-bound transcription factor. *Cell*. **89** (3), 331-340, (1997).  
538 44 Horton, J. D., Goldstein, J. L. & Brown, M. S. SREBPs: activators of the complete program  
539 of cholesterol and fatty acid synthesis in the liver. *The Journal of Clinical Investigation*.  
540 **109** (9), 1125-1131, (2002).  
541 45 Tavintharan, S. *et al.* Reduced mitochondrial coenzyme Q10 levels in HepG2 cells treated  
542 with high-dose simvastatin: A possible role in statin-induced hepatotoxicity? *Toxicology*  
543 *and Applied Pharmacology*. **223** (2), 173-179, (2007).  
544 46 Thomas, E. *et al.* HCV infection induces a unique hepatic innate immune response  
545 associated with robust production of type III interferons. *Gastroenterology*. **142** (4), 978-  
546 988, (2012).  
547 47 Thomas, E. & Liang, T. J. Experimental models of hepatitis B and C—new insights and  
548 progress. *Nature Reviews Gastroenterology & Hepatology*. **13** (6), 362, (2016).  
549 48 Yoneda, M. *et al.* Hepatitis B Virus and DNA Stimulation Trigger a Rapid Innate Immune  
550 Response through NF- $\kappa$ B. *The Journal of Immunology*. 1502677, (2016).  
551

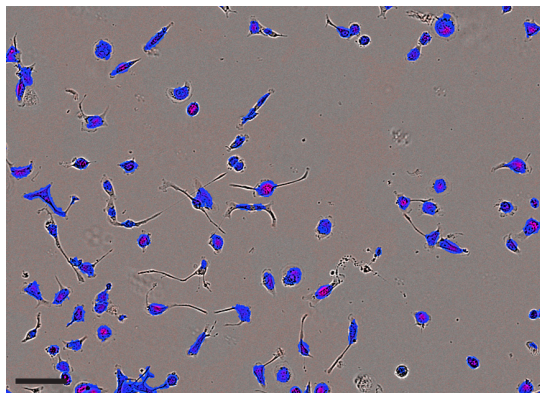
**A**  
UNMASKED



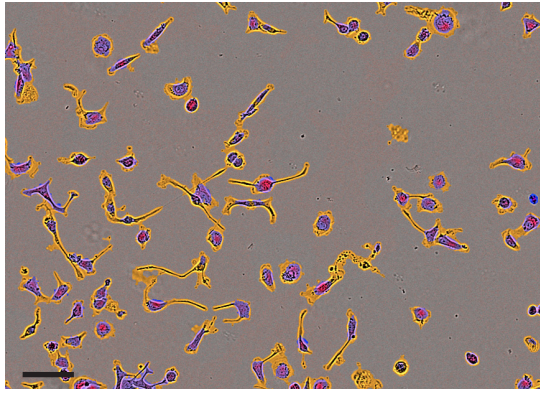
**B**  
PHASE



**C**  
RED OBJECT



**D**  
RED AND PHASE



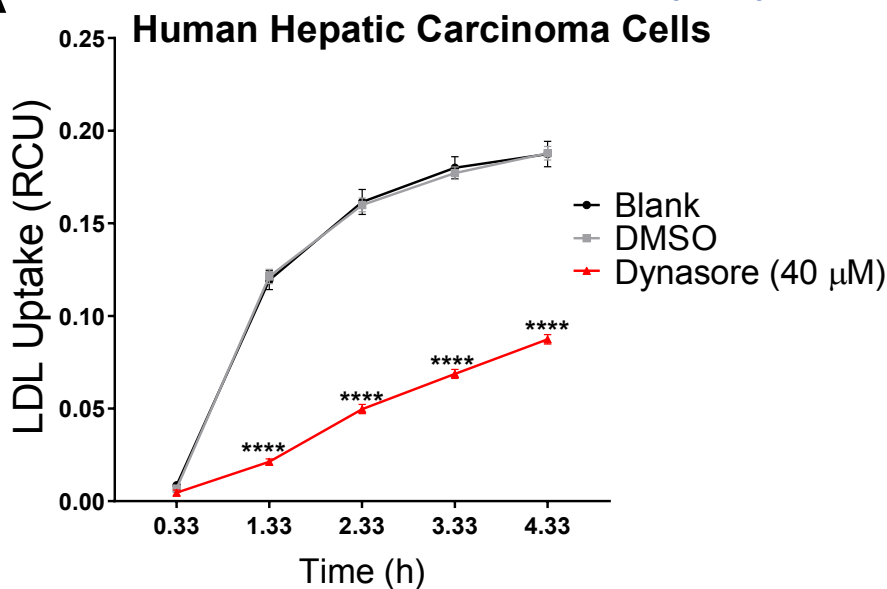
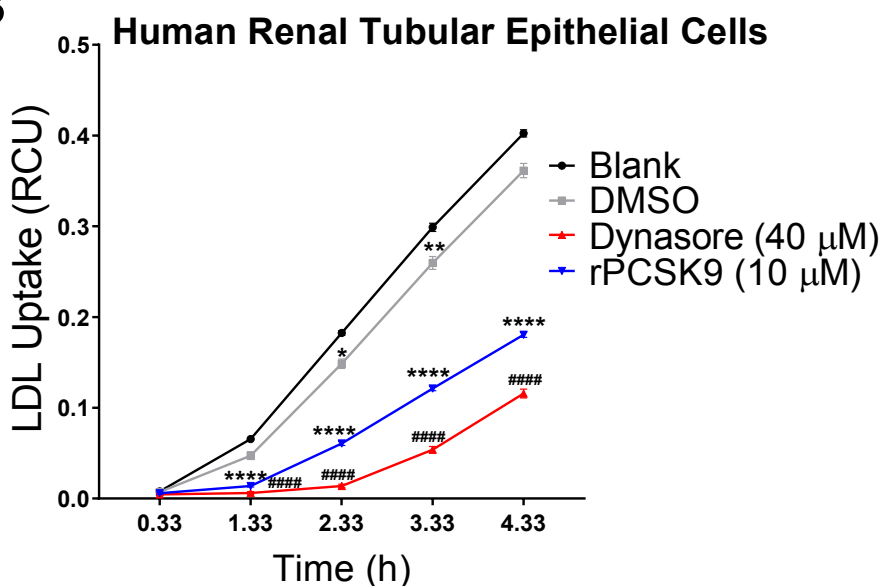
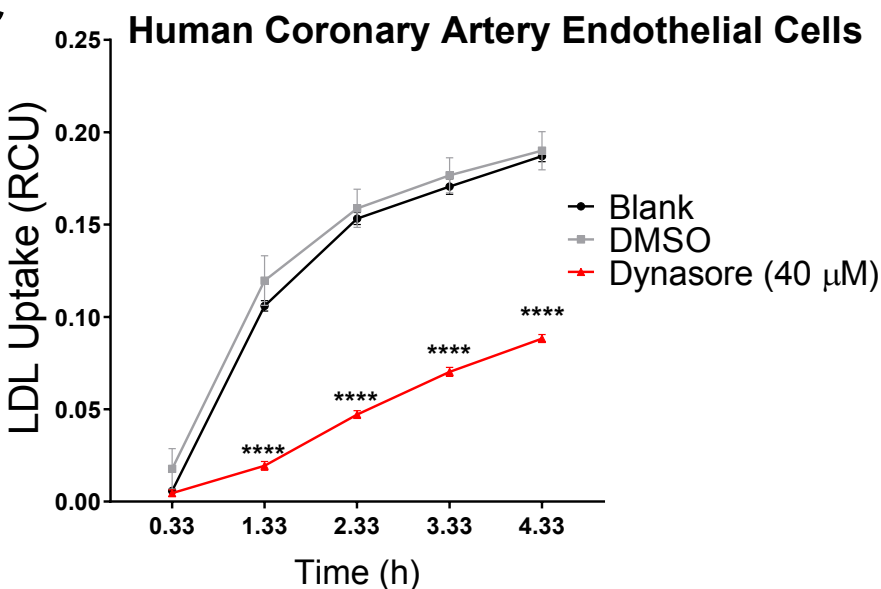
**A****B****C**

Figure 3

[Click here to access/download;Figure;Fig3-Influx graphs with simvastatin over time 8-2-18.pdf](#)

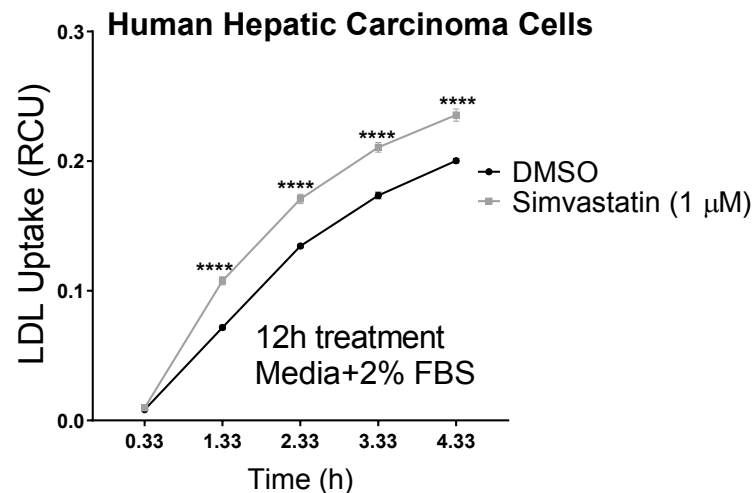
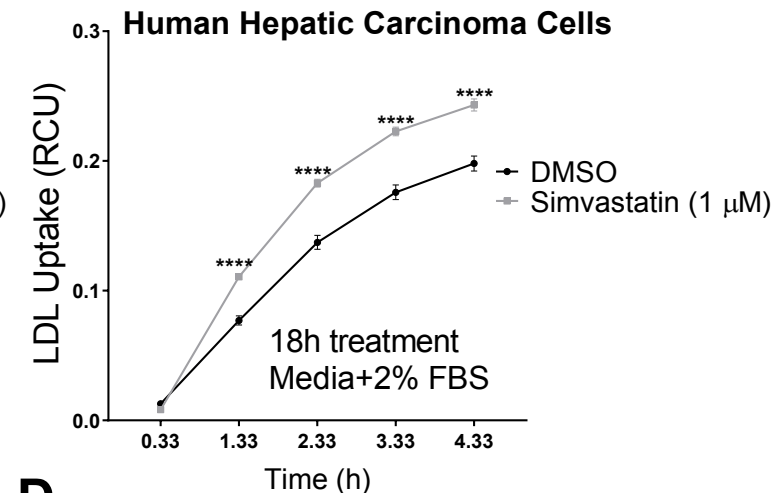
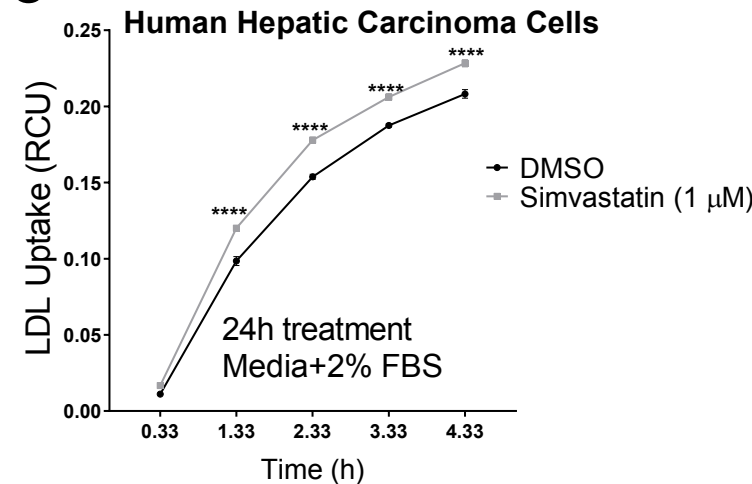
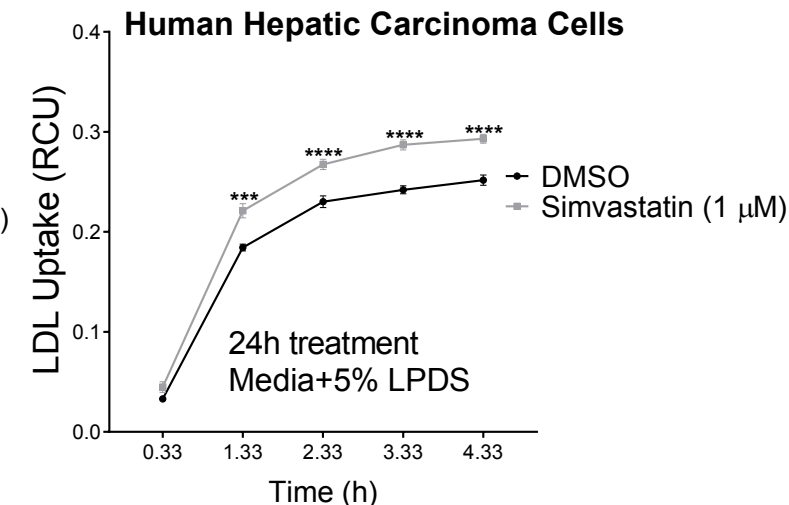
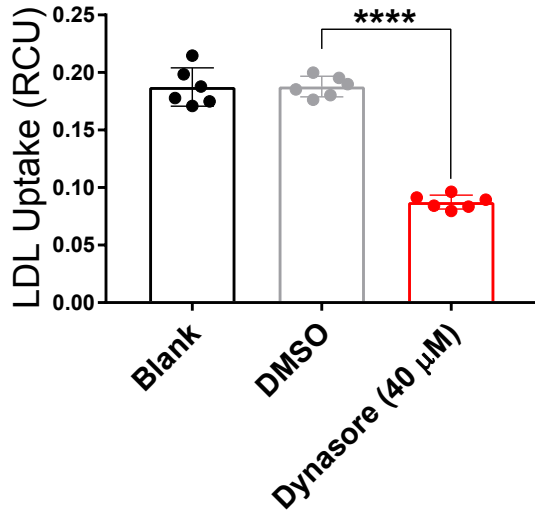
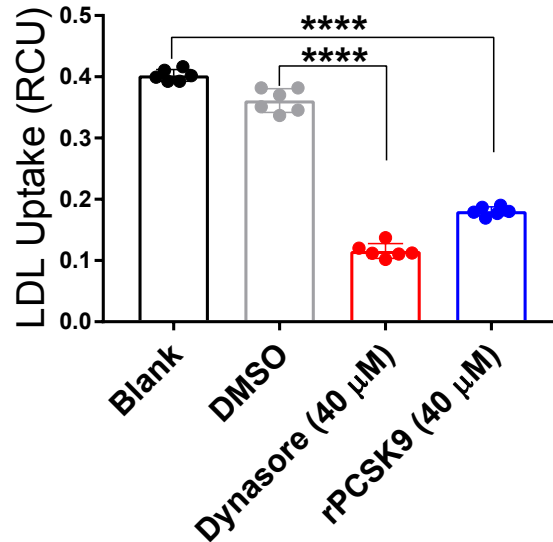
**A****B****C****D**

Figure 4

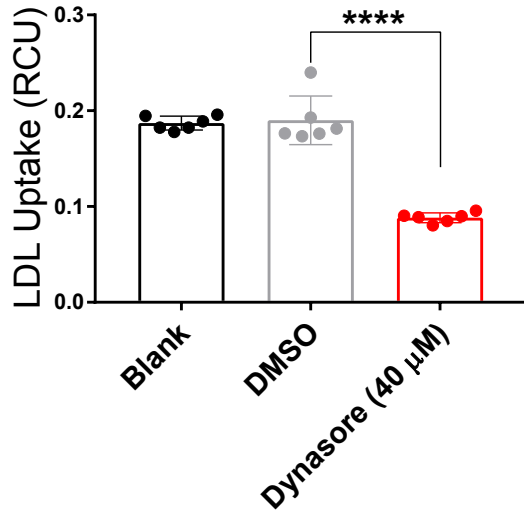
**A** Human Hepatic Carcinoma Cells



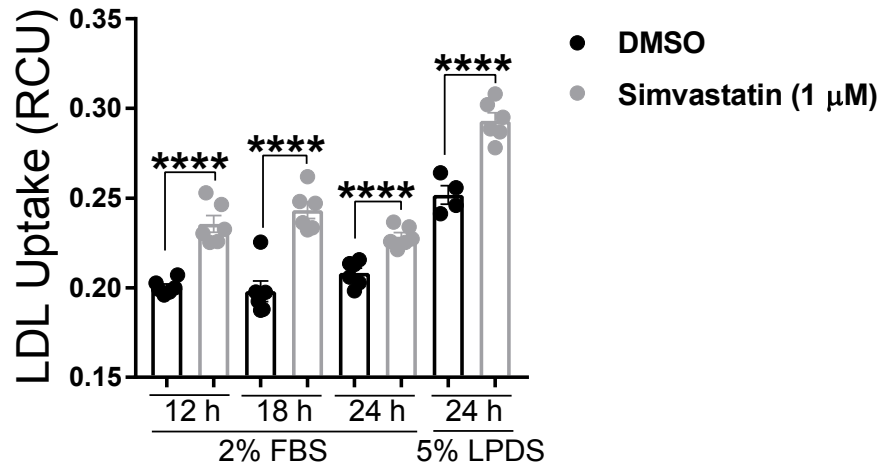
**B** Human Renal Tubular Epithelial Cells



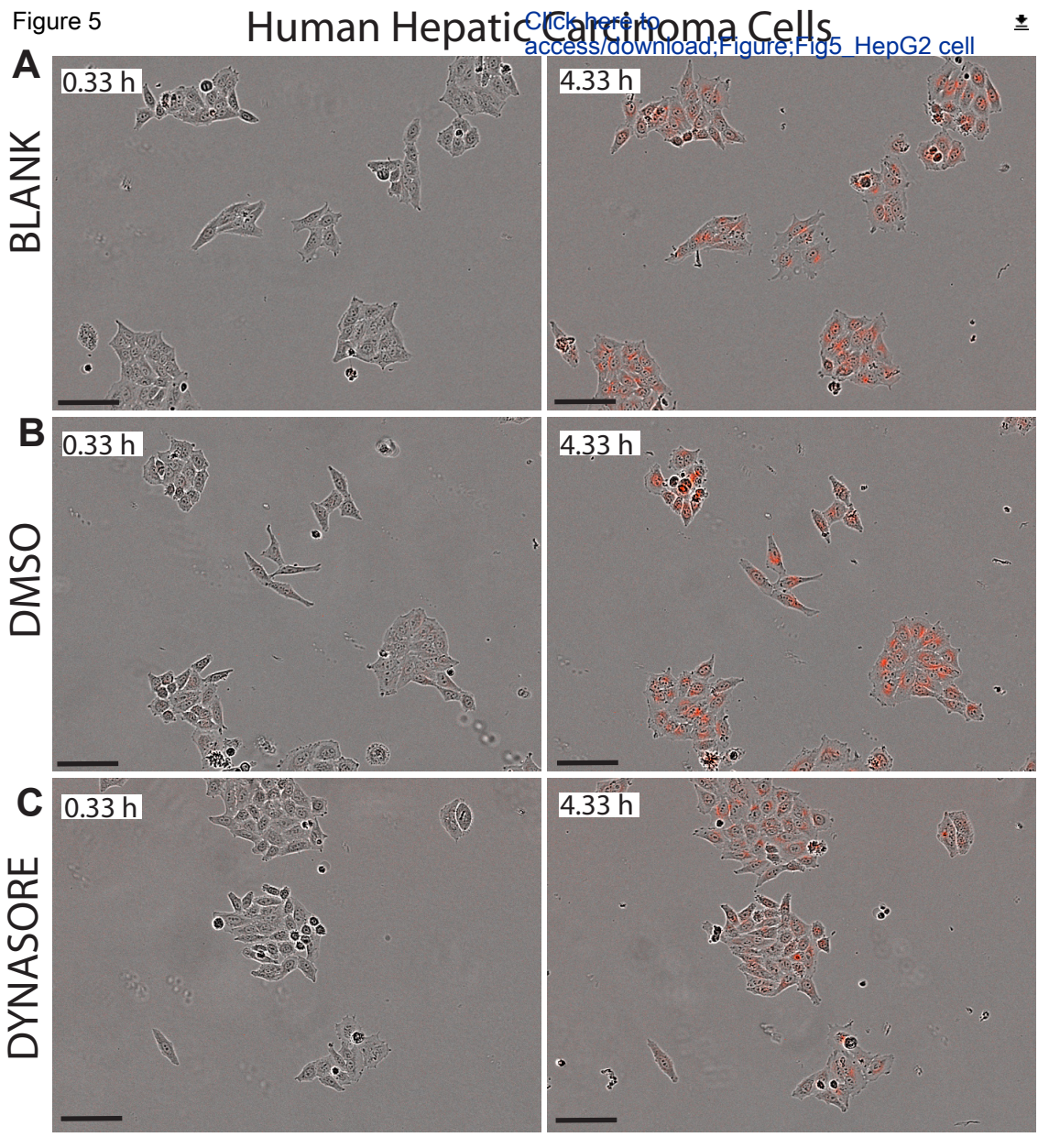
**C** Human Coronary Artery Endothelial Cells



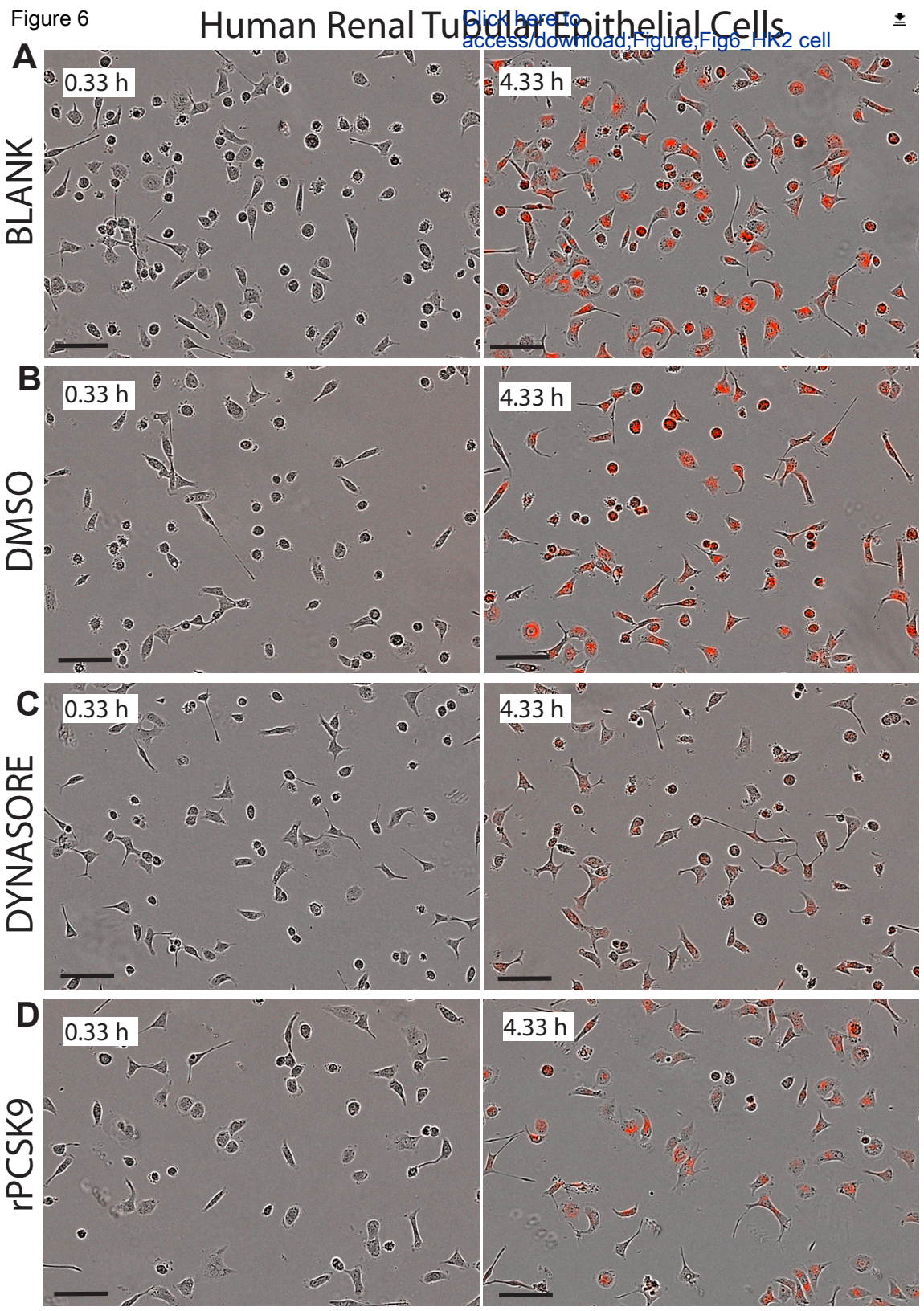
**D** Human Hepatic Carcinoma Cells



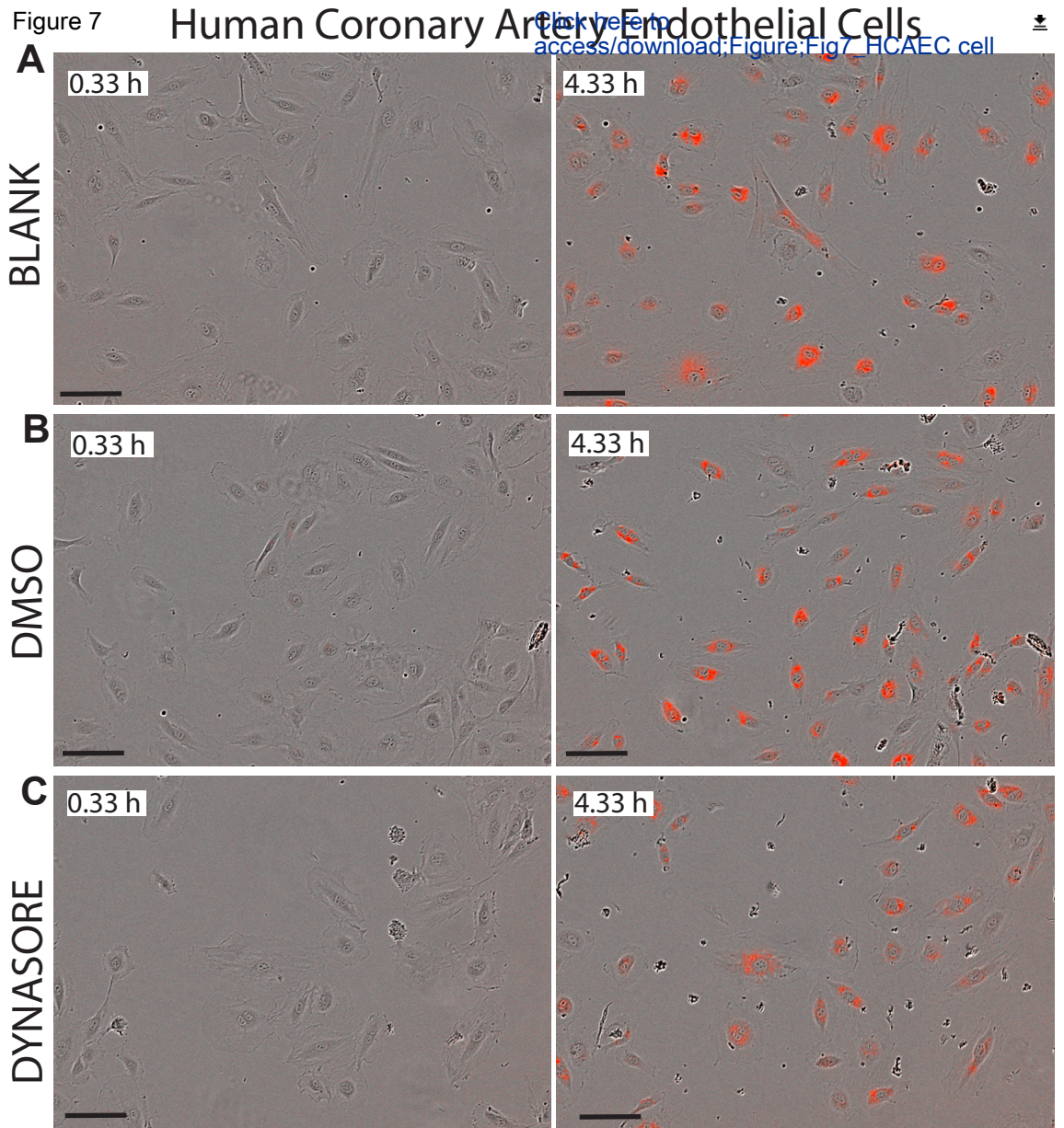












**A. HepG2 Cells**

Elapsed Time (h)	HepG2 + DMSO	HepG2 + Dynasore
1.33	2%	-83%
2.33	-1%	-69%
3.33	-2%	-61%
4.33	0%	-53%

**B. HK2 Cells**

Elapsed Time (h)	HK2 + DMSO	HK2 + Dynasore	HK2 + PCSK9
1.33	-28%	-87%	-79%
2.33	-19%	-91%	-67%
3.33	-13%	-79%	-59%
4.33	-10	-68%	-55%

**C. HCAE Cells**

Elapsed Time (h)	HCAEC + DMSO	HCAEC + Dynasore
1.33	13%	-84%
2.33	4%	-70%
3.33	4%	-60%
4.33	2%	-54%

**D. HepG2 Cells**

Elapsed Time (h)	HepG2 + FBS + Simvastatin 12 h	HepG2 + FBS + Simvastatin 18 h	HepG2 + FBS + Simvastatin 24 h	HepG2 + LPDS + Simvastatin 24 h
1.33	50%	44%	22%	20%
2.33	27%	33%	16%	16%
3.33	21%	27%	10%	19%
4.33	18%	23%	10%	16%

HepG2	HK2	HCAEC
<b>Phase (Analyze)</b> ➤ <i>Parameters:</i> ○ Segmentation adjustment: <b>0.6</b> ➤ <i>Cleanup:</i> ○ Hole fill: <b>0</b> ○ Adjust size: <b>0</b> ➤ <i>Filters:</i> ○ Area (um <sup>2</sup> ): <input checked="" type="checkbox"/> min= <b>1300.0</b> , <input type="checkbox"/> max= <b>1300.0</b> ○ Eccentricity: <b>not selected</b>	<b>Phase (Analyze)</b> ➤ <i>Parameters:</i> ○ Segmentation adjustment: <b>0.6</b> ➤ <i>Cleanup:</i> ○ Hole fill: <b>0</b> ○ Adjust size: <b>0</b> ➤ <i>Filters:</i> ○ Area (um <sup>2</sup> ): <input checked="" type="checkbox"/> min= <b>600.0</b> , <input type="checkbox"/> max= <b>600.0</b> ○ Eccentricity: <b>not selected</b>	<b>Phase (Analyze)</b> ➤ <i>Parameters:</i> ○ Segmentation adjustment: <b>0.6</b> ➤ <i>Cleanup:</i> ○ Hole fill: <b>0</b> ○ Adjust size: <b>0</b> ➤ <i>Filters:</i> ○ Area (um <sup>2</sup> ): <input checked="" type="checkbox"/> min= <b>400.0</b> , <input type="checkbox"/> max= <b>400.0</b> ○ Eccentricity: <b>not selected</b>
<b>Green (Not Selected)</b> <b>Red (Analyze)</b> ➤ <i>Parameters:</i> ○ <b>Top-Hat</b> ○ Radius(um): <b>50</b> ○ Threshold (RCU): <b>0.3</b> ○ Edge Split <b>Off</b> ➤ <i>Cleanup :</i> ○ Hole fill: <b>0</b> ○ Adjust size: <b>0</b> ➤ <i>Filters:</i> ○ Area (um <sup>2</sup> ): <input checked="" type="checkbox"/> min= <b>96.0</b> , <input type="checkbox"/> max= <b>96.0</b> ○ Eccentricity: <b>not selected</b> ○ Mean Intensity: <b>not selected</b> ○ Integrated Intensity: <b>not selected</b>	<b>Green (Not Selected)</b> <b>Red (Analyze)</b> ➤ <i>Parameters:</i> ○ <b>Top-Hat</b> ○ Radius(um): <b>50</b> ○ Threshold (RCU): <b>0.3</b> ○ Edge Split <b>Off</b> ➤ <i>Cleanup :</i> ○ Hole fill: <b>0</b> ○ Adjust size: <b>0</b> ➤ <i>Filters:</i> ○ Area (um <sup>2</sup> ): <input checked="" type="checkbox"/> min= <b>96.0</b> , <input type="checkbox"/> max= <b>96.0</b> ○ Eccentricity: <b>not selected</b> ○ Mean Intensity: <b>not selected</b> ○ Integrated Intensity: <b>not selected</b>	<b>Green (Not Selected)</b> <b>Red (Analyze)</b> ➤ <i>Parameters:</i> ○ <b>Top-Hat</b> ○ Radius(um): <b>50</b> ○ Threshold (RCU): <b>0.3</b> ○ Edge Split <b>Off</b> ➤ <i>Cleanup :</i> ○ Hole fill: <b>0</b> ○ Adjust size: <b>0</b> ➤ <i>Filters:</i> ○ Area (um <sup>2</sup> ): <input checked="" type="checkbox"/> min= <b>96.0</b> , <input type="checkbox"/> max= <b>96.0</b> ○ Eccentricity: <b>not selected</b> ○ Mean Intensity: <b>not selected</b> ○ Integrated Intensity: <b>not selected</b>

Name	Company
pHrodo Red-LDL	ThermoFisher Scientific
HepG2 cells	E. Thomas Lab, U. Miami
MEM	Sigma
Sodium Pyruvate	Sigma
L-Glutamine 200mM solution	Sigma
FBS	Atlas Biologicals
HK2 cells	ATCC
Keratinocyte SFM media kit	Gibco
Primary Coronary Artery Endothelial Cells	ATCC
Vascular Cell Basal Medium	ATCC
Endothelial Cell Growth Kit-VEGF	ATCC
Human Lipoprotein Deficient Serum	Millipore
PBS	Sigma
Trypsin-EDTA (0.25%)	Gibco
Trypsin-EDTA (0.05%)	Gemini Bio-Products
Trypsin Neutralizing Solution	ATCC
24 well plate	Falcon
40 $\mu$ M mesh cell strainer	VWR
15 mL conical tubes	VWR
50 mL conical tubes	VWR
Trypan Blue Staining (0.4%)	Life Technologies
Counting Slides	Bio-Rad
Incucyte Zoom	Sartorius
Dynasore Hydrate	Sigma
PCSK9 Recombinant Protein	Cayman Chemicals

Catalog Number	Comments
L34356	
HB-8065	
M0325	
P5280	
G7513	
FP-0500-A	
CRL-2190	
17005-042	
PCS-100-020	
PCS-100-030	
PCS-100-041	
LP4	
D8537	
25200056	
400-150	
PCS-999-004	
353226	
10199-654	
89039-666	
89039-658	
T10282	
145-0011	
Zoom	Imaging and analysis platform
D7693	
20631	



1 Alewife Center #200  
Cambridge, MA 02140  
Tel: 617.945.9051  
www.jove.com

## ARTICLE AND VIDEO LICENSE AGREEMENT

Title of Article:

LDL Cholesterol Uptake Assay Using Live Cell Imaging Analysis with Cell Health Monitoring

Author(s):

Portia Ritter, Keyvan Yousefi, Julian Ramirez, Derek Dykxhoorn, Armand Perez  
and Lina A Shekadeh

Item 1 (check one box): The Author elects to have the Materials be made available (as described at

<http://www.jove.com/author>) via: ☐ Standard Access ☒ Open Access

Item 2 (check one box):



The Author is NOT a United States government employee.



The Author is a United States government employee and the Materials were prepared in the course of his or her duties as a United States government employee.



The Author is a United States government employee but the Materials were NOT prepared in the course of his or her duties as a United States government employee.

### ARTICLE AND VIDEO LICENSE AGREEMENT

1. **Defined Terms.** As used in this Article and Video License Agreement, the following terms shall have the following meanings: "**Agreement**" means this Article and Video License Agreement; "**Article**" means the article specified on the last page of this Agreement, including any associated materials such as texts, figures, tables, artwork, abstracts, or summaries contained therein; "**Author**" means the author who is a signatory to this Agreement; "**Collective Work**" means a work, such as a periodical issue, anthology or encyclopedia, in which the Materials in their entirety in unmodified form, along with a number of other contributions, constituting separate and independent works in themselves, are assembled into a collective whole; "**CRC License**" means the Creative Commons Attribution-Non Commercial-No Derivs 3.0 Unported Agreement, the terms and conditions of which can be found at: <http://creativecommons.org/licenses/by-nc-nd/3.0/legalcode>; "**Derivative Work**" means a work based upon the Materials or upon the Materials and other pre-existing works, such as a translation, musical arrangement, dramatization, fictionalization, motion picture version, sound recording, art reproduction, abridgment, condensation, or any other form in which the Materials may be recast, transformed, or adapted; "**Institution**" means the institution, listed on the last page of this Agreement, by which the Author was employed at the time of the creation of the Materials; "**JoVE**" means MyJoVE Corporation, a Massachusetts corporation and the publisher of *The Journal of Visualized Experiments*; "**Materials**" means the Article and / or the Video; "**Parties**" means the Author and JoVE; "**Video**" means any video(s) made by the Author, alone or in conjunction with any other parties, or by JoVE or its affiliates or agents, individually or in collaboration with the Author or any other parties, incorporating all or any portion of the Article, and in which the Author may or may not appear.

2. **Background.** The Author, who is the author of the Article, in order to ensure the dissemination and protection of the Article, desires to have the JoVE publish the Article and create and transmit videos based on the Article. In furtherance of such goals, the Parties desire to memorialize in this Agreement the respective rights of each Party in and to the Article and the Video.

3. **Grant of Rights in Article.** In consideration of JoVE agreeing to publish the Article, the Author hereby grants to JoVE, subject to **Sections 4 and 7** below, the exclusive, royalty-free, perpetual (for the full term of copyright in the Article, including any extensions thereto) license (a) to publish, reproduce, distribute, display and store the Article in all forms, formats and media whether now known or hereafter developed (including without limitation in print, digital and electronic form) throughout the world, (b) to translate the Article into other languages, create adaptations, summaries or extracts of the Article or other Derivative Works (including, without limitation, the Video) or Collective Works based on all or any portion of the Article and exercise all of the rights set forth in (a) above in such translations, adaptations, summaries, extracts, Derivative Works or Collective Works and (c) to license others to do any or all of the above. The foregoing rights may be exercised in all media and formats, whether now known or hereafter devised, and include the right to make such modifications as are technically necessary to exercise the rights in other media and formats. If the "Open Access" box has been checked in **Item 1** above, JoVE and the Author hereby grant to the public all such rights in the Article as provided in, but subject to all limitations and requirements set forth in, the CRC License.



## ARTICLE AND VIDEO LICENSE AGREEMENT

4. **Retention of Rights in Article.** Notwithstanding the exclusive license granted to JoVE in **Section 3** above, the Author shall, with respect to the Article, retain the non-exclusive right to use all or part of the Article for the non-commercial purpose of giving lectures, presentations or teaching classes, and to post a copy of the Article on the Institution's website or the Author's personal website, in each case provided that a link to the Article on the JoVE website is provided and notice of JoVE's copyright in the Article is included. All non-copyright intellectual property rights in and to the Article, such as patent rights, shall remain with the Author.

5. **Grant of Rights in Video – Standard Access.** This **Section 5** applies if the "Standard Access" box has been checked in **Item 1** above or if no box has been checked in **Item 1** above. In consideration of JoVE agreeing to produce, display or otherwise assist with the Video, the Author hereby acknowledges and agrees that, Subject to **Section 7** below, JoVE is and shall be the sole and exclusive owner of all rights of any nature, including, without limitation, all copyrights, in and to the Video. To the extent that, by law, the Author is deemed, now or at any time in the future, to have any rights of any nature in or to the Video, the Author hereby disclaims all such rights and transfers all such rights to JoVE.

6. **Grant of Rights in Video – Open Access.** This **Section 6** applies only if the "Open Access" box has been checked in **Item 1** above. In consideration of JoVE agreeing to produce, display or otherwise assist with the Video, the Author hereby grants to JoVE, subject to **Section 7** below, the exclusive, royalty-free, perpetual (for the full term of copyright in the Article, including any extensions thereto) license (a) to publish, reproduce, distribute, display and store the Video in all forms, formats and media whether now known or hereafter developed (including without limitation in print, digital and electronic form) throughout the world, (b) to translate the Video into other languages, create adaptations, summaries or extracts of the Video or other Derivative Works or Collective Works based on all or any portion of the Video and exercise all of the rights set forth in (a) above in such translations, adaptations, summaries, extracts, Derivative Works or Collective Works and (c) to license others to do any or all of the above. The foregoing rights may be exercised in all media and formats, whether now known or hereafter devised, and include the right to make such modifications as are technically necessary to exercise the rights in other media and formats. For any Video to which this Section 6 is applicable, JoVE and the Author hereby grant to the public all such rights in the Video as provided in, but subject to all limitations and requirements set forth in, the CRC License.

7. **Government Employees.** If the Author is a United States government employee and the Article was prepared in the course of his or her duties as a United States government employee, as indicated in **Item 2** above, and any of the licenses or grants granted by the Author hereunder exceed the scope of the 17 U.S.C. 403, then the rights granted hereunder shall be limited to the maximum rights permitted under such

statute. In such case, all provisions contained herein that are not in conflict with such statute shall remain in full force and effect, and all provisions contained herein that do so conflict shall be deemed to be amended so as to provide to JoVE the maximum rights permissible within such statute.

8. **Likeness, Privacy, Personality.** The Author hereby grants JoVE the right to use the Author's name, voice, likeness, picture, photograph, image, biography and performance in any way, commercial or otherwise, in connection with the Materials and the sale, promotion and distribution thereof. The Author hereby waives any and all rights he or she may have, relating to his or her appearance in the Video or otherwise relating to the Materials, under all applicable privacy, likeness, personality or similar laws.

9. **Author Warranties.** The Author represents and warrants that the Article is original, that it has not been published, that the copyright interest is owned by the Author (or, if more than one author is listed at the beginning of this Agreement, by such authors collectively) and has not been assigned, licensed, or otherwise transferred to any other party. The Author represents and warrants that the author(s) listed at the top of this Agreement are the only authors of the Materials. If more than one author is listed at the top of this Agreement and if any such author has not entered into a separate Article and Video License Agreement with JoVE relating to the Materials, the Author represents and warrants that the Author has been authorized by each of the other such authors to execute this Agreement on his or her behalf and to bind him or her with respect to the terms of this Agreement as if each of them had been a party hereto as an Author. The Author warrants that the use, reproduction, distribution, public or private performance or display, and/or modification of all or any portion of the Materials does not and will not violate, infringe and/or misappropriate the patent, trademark, intellectual property or other rights of any third party. The Author represents and warrants that it has and will continue to comply with all government, institutional and other regulations, including, without limitation all institutional, laboratory, hospital, ethical, human and animal treatment, privacy, and all other rules, regulations, laws, procedures or guidelines, applicable to the Materials, and that all research involving human and animal subjects has been approved by the Author's relevant institutional review board.

10. **JoVE Discretion.** If the Author requests the assistance of JoVE in producing the Video in the Author's facility, the Author shall ensure that the presence of JoVE employees, agents or independent contractors is in accordance with the relevant regulations of the Author's institution. If more than one author is listed at the beginning of this Agreement, JoVE may, in its sole discretion, elect not take any action with respect to the Article until such time as it has received complete, executed Article and Video License Agreements from each such author. JoVE reserves the right, in its absolute and sole discretion and without giving any reason therefore, to accept or decline any work submitted to JoVE. JoVE and its employees, agents and independent contractors shall have

## ARTICLE AND VIDEO LICENSE AGREEMENT

full, unfettered access to the facilities of the Author or of the Author's institution as necessary to make the Video, whether actually published or not. JoVE has sole discretion as to the method of making and publishing the Materials, including, without limitation, to all decisions regarding editing, lighting, filming, timing of publication, if any, length, quality, content and the like.

11. **Indemnification.** The Author agrees to indemnify JoVE and/or its successors and assigns from and against any and all claims, costs, and expenses, including attorney's fees, arising out of any breach of any warranty or other representations contained herein. The Author further agrees to indemnify and hold harmless JoVE from and against any and all claims, costs, and expenses, including attorney's fees, resulting from the breach by the Author of any representation or warranty contained herein or from allegations or instances of violation of intellectual property rights, damage to the Author's or the Author's institution's facilities, fraud, libel, defamation, research, equipment, experiments, property damage, personal injury, violations of institutional, laboratory, hospital, ethical, human and animal treatment, privacy or other rules, regulations, laws, procedures or guidelines, liabilities and other losses or damages related in any way to the submission of work to JoVE, making of videos by JoVE, or publication in JoVE or elsewhere by JoVE. The Author shall be responsible for, and shall hold JoVE harmless from, damages caused by lack of sterilization, lack of cleanliness or by contamination due to the making of a video by JoVE its employees, agents or independent contractors. All sterilization, cleanliness or decontamination procedures shall be solely the responsibility of the Author and shall be undertaken at the Author's

expense. All indemnifications provided herein shall include JoVE's attorney's fees and costs related to said losses or damages. Such indemnification and holding harmless shall include such losses or damages incurred by, or in connection with, acts or omissions of JoVE, its employees, agents or independent contractors.

12. **Fees.** To cover the cost incurred for publication, JoVE must receive payment before production and publication the Materials. Payment is due in 21 days of invoice. Should the Materials not be published due to an editorial or production decision, these funds will be returned to the Author. Withdrawal by the Author of any submitted Materials after final peer review approval will result in a US\$1,200 fee to cover pre-production expenses incurred by JoVE. If payment is not received by the completion of filming, production and publication of the Materials will be suspended until payment is received.

13. **Transfer, Governing Law.** This Agreement may be assigned by JoVE and shall inure to the benefits of any of JoVE's successors and assignees. This Agreement shall be governed and construed by the internal laws of the Commonwealth of Massachusetts without giving effect to any conflict of law provision thereunder. This Agreement may be executed in counterparts, each of which shall be deemed an original, but all of which together shall be deemed to me one and the same agreement. A signed copy of this Agreement delivered by facsimile, e-mail or other means of electronic transmission shall be deemed to have the same legal effect as delivery of an original signed copy of this Agreement.

A signed copy of this document must be sent with all new submissions. Only one Agreement required per submission.

### CORRESPONDING AUTHOR:

Name:

Lina A Shehadeh

Department:

Medicine

Institution:

University of Miami - Miller School of Medicine

Article Title:

LDL cholesterol Uptake Assay Using Live Cell Imaging Analysis with Cell Health Monitoring

Signature:

Lina Shehadeh

Digitally signed by Lina Shehadeh  
DN: cn=Lina Shehadeh, o=University of  
Miami, ou=PhD,  
email=lshehadeh@med.miami.edu, c=US  
Date: 2018.06.01 12:36:25 -04'00'

Date:

Please submit a signed and dated copy of this license by one of the following three methods:

- 1) Upload a scanned copy of the document as a pdf on the JoVE submission site;
- 2) Fax the document to +1.866.381.2236;
- 3) Mail the document to JoVE / Attn: JoVE Editorial / 1 Alewife Center #200 / Cambridge, MA 02139

For questions, please email [submissions@jove.com](mailto:submissions@jove.com) or call +1.617.945.9051

Dear editor,

Please see responses to your comments below.

1. It's fine that you focus on the IncuCyte system here, but do you have specific alternatives you can recommend in the manuscript?

We added to the Discussion the following:

“While this protocol offers specifications for IncuCyte live imaging and analysis system, the protocol can be adapted for alternative imaging systems such as Cellomics.”

2. Figure 3: There do not appear to be any ‘####’ markings in the Figure itself.

Fixed.

3. The uploaded figure 4 is incorrect.

Fixed.

4. Table 1: Note that Tables will be formatted directly from the excel files for web viewing, and therefore certain formatting choices and special characters may not be displayed correctly. Could this be a Figure instead?

Please continue to use the excel file. We can also send you the table as a pdf but would rather present it as a table instead. Can you please let us know if and which characters would be affected? Please let us know. Thanks.

5. Table 2: There is no ‘D’ in the table.

Added.